Construction of heterojunction superparamagnetic $Cd_{0.5}Ag_{0.5}Fe_2O_4$ nanocomposite photocatalyst for simulated textile effluent oxidation

Journal of Physics: Conference Series **2830** (2024) 012018 doi:10.1088/1742-6596/2830/1/012018

Construction of heterojunction superparamagnetic $Cd_{0.5}Ag_{0.5}Fe_2O_4$ nanocomposite photocatalyst for simulated textile effluent oxidation

Ahmed H. Mangood[1], Eman Sh. Salama [1,2*], Ibrahim E.T. El-Sayed[1]; Mai K. Fouad[3], MA. Tony[2]

[1]Chemistry department, Faculty of Science, Menoufia University, Shebin El-Kom, Egypt.
[2]Advanced Materials/Solar Energy and Environmental Sustainability (AMSEES) Laboratory, Basic Engineering Science Department, Faculty of Engineering, Menoufia University, Shebin El-Kom, Egypt.
[3]Chemical Engineering Department, Faculty of Engineering, Cairo University, Egypt.

emanshaban277@gmail.com

Abstract. Significant attempts have been recently made regarding nanomaterials due to their several environmental applications especially in wastewater treatment technologies. Among the available nanoparticles, ferrite based substances are gaining a special interest since their superior characteristics such as their magnetic nature, high adsorption capacity and large specific surface area. In this regard, $Cd_{0.5}Ag_{0.5}Fe_2O_4$ was prepared using the green simple co-precipitation route. Then, the sample is characterized via Scanning Electron Microscopy (SEM) that proved the produced material's surface morphology. The substance is then employed as a catalyst source for Fenton reaction to oxidize textile effluent solution containing Rhodamine B (Rh-B 6G) dye. The oxidation experiment conducted under ultraviolet (UV) light with the ferrite-based Fenton catalyst supplemented with hydrogen peroxide showed an exceptional removal rate of up to 94% removals. Notably, the oxidation system is significantly impacted by the operational variables. The oxidation efficiency of the dye was maximized at pH 3.0 and 50 mg/L and 1600 mg/L for ferrite-based Fenton catalyst and H_2O_2, respectively. The impacts of the operational factors, i.e. initial pH value, initial dye concentration, catalyst, and H_2O_2 concentrations were also investigated. This perspective introduces the role of a superparamagnetic material to be a recyclable sustained catalyst.

1. Introduction

Textile wastewater contaminated with dye effluents is signified as one of the main issues in the modern societies. [1]. Around 700,000 numerous kinds of dyes are generated from such industries. As a result, serious health concerns are being raised due to the majority of them are disposed onto the nearby watercourse, which is still need treatment and purification [2]. Basic dye rhodamine-B 6G (Rh-B 6G) is widely applied in various industries including those that produce leather, textiles, paper products, food, and pharmaceuticals. RhB's dye possesses an aromatic structure and xanthene ring, which are signified,

as difficult to break down. On the other hand they block light penetration, thus they also inhibit photosynthesis in aquatic plants that might be harmful to the ecosystem [3]. Nevertheless, rhodamine B is carcinogenic by nature, which leads to major issues for humans, environment and biology system. In this regard, it's essential to eliminate it from ecosystem [2].

Recent research advances is dealing with the elimination of dangerous and cancer-causing dye-based pollutants from industrial wastewater. Such techniques including physical, chemical and biological methods have been extensively employed to address such wastewater contaminations [4]. The most efficient method for the oxidative destruction of organic contaminants, among others, is the use of advanced oxidation processes (AOPs). The generation of extremely reactive oxygen species (ROS) by AOPs, such as radical hydroxyl (·OH), may play a role in the non-selective destruction of many organic pollutants into less hazardous and even non-toxic compounds (H_2O and CO_2) [5]. The presence of Fe^{3+}/Fe^{2+} ions and H_2O_2 can react to generate hydroxyl radical and the reaction is well known as Fenton system. Furthermore, H_2O_2 acts as an oxidizing agent while $Fe^{3+/}Fe^{2+}$ act as a catalyst [6]. The treatment of water by photocatalysis has drawn a numerous interest including its high performance, ability to operate at room temperature and pressure, affordability and lack of secondary waste generation; this technology is crucial for the treatment of water [7]. The catalyst could not be recovered during treatment, hence it is important to emphasize that the homogenous Fenton's system still lacks sustainability.

The photocatalytic qualities of spinel ferrite nanoparticles are useful for a number of processes that might oxidize organic pollutants in wastewater. Spinel ferrite nanoparticles have the general formula AFe_2O_4 (where A might be Zn, Mg, Ni, Mn, etc.), the metal cations A and Fe occupy the tetrahedral and octahedral positions, respectively [6]. Due to high resistivity, low magnetic loss, and high permeability, Cd–Fe mixed ferrites are technically important and suitable for electrical switches. The electrical and magnetic characteristics of ferrites were improved by sparingly adding foreign ion species. Ag^+ ion was often selected among various dopants. Ag was the important noble metal used as a catalyst in industrial catalysis processes because it has a low cost and exists in more than one oxidation state. Additionally, silver compounds have been widely used in a variety of processes, including oxidation, isomerization, biological, optical, catalytic and photocatalytic reactions [4]. Keerthana et al. [8] fabricated Ce-doped $CuFe_2O_4$ by hydrothermal route for rhodamine B photocatalytic oxidation. Also, Jamaludin and his co-workers [9] were successfully prepared $Ce_{0.1}Co_xBi_{1-x}Fe_2O_3$ ($0 \leq x \leq 0.2$) using the sol-gel auto-combustion method and applied them for rhodamine B photooxidation. However, according to the authors' knowledge the matrix of $Cd_{0.5}Ag_{0.5}Fe_2O_4$ ferrite as a source of superparamagnetic Fenton's catalyst is not used so far for rhodamine B photo-oxidation. Therefore, this investigation aimed for preparation of $Cd_{0.5}Ag_{0.5}Fe_2O_4$ ferrite, using the simple co-precipitation technique. Then, the produced ferrite nanoparticle was characterized using Scanning Electron microscope (SEM) study. This ferrite was used as a photocatalyst for oxidation of Rhodamine -B 6G (Rh-B 6G) dye. Additionally, the assessment of the photo oxidation parameters including pH, dye loading, H_2O_2 concentration, catalyst dose and operating temperature are conducted as well.

2. Materials and Procedures

2.1 Reagent and chemical substances

Rhodamine B (Rh-B 6G) dye is used as a model pollutant to simulate textile dying effluent. The precursors of cadmium nitrate ($Cd(NO_3)_2.4H_2O$), ferric nitrate ($Fe(NO_3)_3.9H_2O$) and silver nitrate ($AgNO_3$) for nanoparticles preparation and distilled water is applied. The Fenton's reaction is started with 40% w/w hydrogen peroxide (H_2O_2). The pH was adjusted using sodium hydroxide and sulfuric acid. Chemicals of analytical grades are all provided by Sigma-Aldrich. Also, such chemicals are used as supplied with no further purification or treatment.

2.2. Dye solution preparation

Initially, a stock solution of 1000 ppm of the dye solution was created using 1.0 g of Rh-B 6G dye that was dissolved in 1.0 L of distilled water. Then, further dilution is achieved as required according to the required concentration.

2.3. Experimental methodology

2.3.1 $Cd_{0.5}Ag_{0.5}Fe_2O_4$ ferrite preparation: $Cd_{0.5}Ag_{0.5}Fe_2O_4$ ferrite was prepared by a simple co-precipitation route using cadmium nitrate, silver nitrate and ferric nitrate. These nitrate salts were dissolved in distilled water with1:2 molar ratios. Then, the precipitate formed by adding (3.0 mol L^{-1}) of sodium hydroxide drop by drop. For two hours, the solution combination was constantly agitated at 80 °C. The sample was subjected for repetitive washing with distilled water and magnetically decanted to produce soft ferrite particles. The attained powered is then exposed for overnight oven drying at 80 °C. Then the attained sample is subjected for surface morphology to examine the particles via field emission scanning electron microscopy (FESEM) instrument (SU8000 Type II, Hitachi).

2.3.2. Photocatalytic methodology: Preliminary, the prepared synthetic Rhodamine-B 6G (Rh-B 6G) is diluted as needed. A 100 mL of a certain concentration of the prepared aqueous solution is used for the photo-oxidation process. A digital pH meter (AD1030, Adwa digital pH-meter instrument, Hungary) is then used to alter the pH value of the solution, if necessary, using diluted NaOH and/or H_2SO_4 solutions. Hydrogen peroxide (H_2O_2) is added to the heterogeneous mixture after the nanoparticles have been introduced, starting the Fenton reaction. The combination is then exposed to ultraviolet light using a 12-watt UV lamp. Afterwards, a micro filter (0.45 μm) is used to subject the solution to catalyst isolation prior to the periodic examination using a UV-1601, Shimadzu, Model TCC-240A, Japan, spectrophotometer that has been adjusted to the highest wavelength of the dye under investigation (554 nm wavelength).

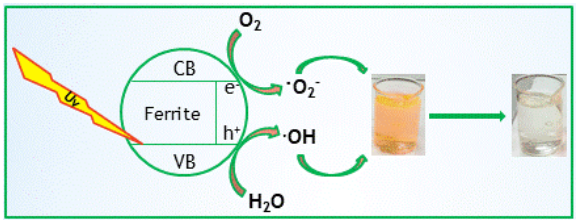

Figure 1. Diagram schematic of the lab-scale photo-Fenton for the removal of (Rh-B 6G).

3. Result and discussion

3.1 Scanning Electron Microscopy (SEM)

The morphological examination of the produced ferrite was examined using Scanning Electron Microscope (SEM). It was found from Fig. 2 that, such nanoparticles of ferrite is representing a spherical shape with a narrow size distribution, and the grain size was found to be 44.33 nm. The narrow grain size distribution of magnetite is correlated with the spherical shape of the nanoparticles [10]. Also, the image displays an agglomeration between the particles indicating the magnetic nature of the prepared ferrite. Such magnetic nature enables the particles for the easiness separation and sustainable reuse [6].

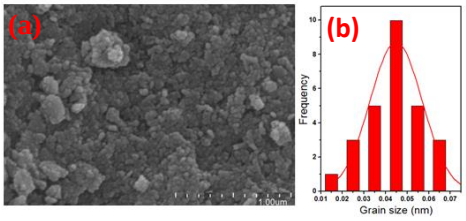

Figure 2. (a) SEM image and (b) Histogram of the grain size distribution of $Cd_{0.5}Ag_{0.5}Fe_2O_4$ nanoparticles.

3.2 Comparing various oxidation systems

Appling various oxidation systems are applied for Rh-B 6G dye elimination. AS shown in Fig. 3, the solo ferrite catalyst augmented with Ultraviolet illumination (UV) oxidizes only 42.54 % of Rh-B 6G dye during the first 60 minutes of illumination. But, 39.22 % removal is achieved when H_2O_2 (400 mg/L) is used in conjunction with UV light. This is connected to ·OH radicals generation in the reaction

solution when H_2O_2 was added. These radicals are the most oxidative for the dye molecules that attack them and destruction of their aromatic rings. Thus, the dye is oxidized and the intermediates of the reaction are ultimately turned into the end products, which are CO_2 and H_2O, which are harmless. However, a higher removal effectiveness of 96.68% is achieved by adding 50 and 1600 mg/L of ferrite nanoparticles and H_2O_2, respectively, which represent Fenton's reagents under UV irradiation. This might be because the dual treatment systems, which increase the formation of •OH and, as a result, attain a higher oxidation rate. This outcome is consistent with the earlier study [11].

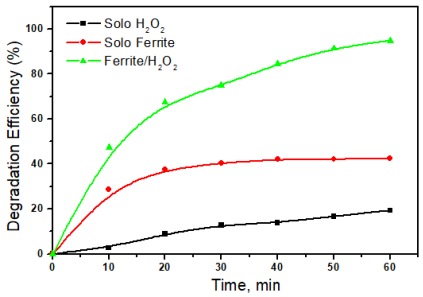

Figure 3. Comparing the effects of several oxidation systems on the dye removal of Rh-B 6G.

3.3 The impact of the photo-Fenton parameters

3.3.1 Effect of pH: The pH value has a major effect on the Fenton reaction efficiency since it influences the reaction between H_2O_2 and iron species, which in turn influences the formation of OH radicals. To examine the pH effect, ferrite (50 mg/L) and H_2O_2 (1600 mg/L) concentrations were kept constant, and the initial pH values were adjusted between 3.0 and 8.0 [11]. There is a 94.85% removal of (Rh-B 6G) within 60 minutes of reaction time at the optimal pH-value 3.0. On the other hand, the removal of this dye is 82.85% at pH 8.0. The highest possible generation of •OH radicals in the acidic medium is most likely the cause of this observation. The acidic medium contains an organometallic complex as well, which may facilitate H_2O_2 regeneration. Instead of •OH radicals, unfavorable radicals are produced at high pH levels [12]. Also Rhodamine dye is cationic dye so on alkaline solution the surface of photocatalyst carry negative charge and there was attraction between it and the cationic dye, so the removal efficiency increase at pH 8.0 [13].

3.3.2. Effect of dosage of ferrite catalyst: For Fenton's oxidation system, four tests were carried out at different ferrite concentrations ranging from 20 to 100 mg/L to establish the optimal catalyst dose. Nevertheless, all other parameters remain unchanged, including the original (Rh-B 6G) dye concentration of 10 ppm, 1600 mg/L H_2O_2, and pH of 3.0. According to the data shown in Fig. 4b, the ideal concentration of this ferrite is 50 mg/L, which corresponds to 94.85% oxidation. This is due to the fact that the generated active species in the reaction medium is enough to oxidize the dye. But, as the catalyst load increased, the active sites decreased as a result of the particles aggregating and preventing the catalyst's surface from being exposed to UV light. Thereby, the catalytic activity is deduced and the result is a decrease in the oxidation rate. This might be leading to a Fenton's oxidation deficiency. This is consistent with the earlier research that was documented in the literature [14].

3.3.3. Hydrogen peroxide dosage's effects: The concentration of hydrogen peroxide is one of the key parameters in the Fenton's reaction system. This is due to the optimal hydrogen peroxide dose is essential for the maximum OH radicals' generation. In this regard, to evaluate the optimal hydrogen peroxide dose, all other parameters are kept constant (pH 3.0, 10 ppm dye and 50 mg/L of ferrite catalyst). The effect of increasing the hydrogen peroxide concentration on the rate of (Rh-B 6G) reduction is seen in Fig. 4d. The study examined a variety of initial H_2O_2 values, from 400 to 3200 mg/L. The plot displayed in Fig. 4d demonstrates that the overall dye removal increases when the H_2O_2 concentration is exceeded. But this is accepted a certain limit (until a concentration of 1600 mg/L). Extra peroxide dose supplemented to the reaction media decreasing the oxidation efficiency. This might

be due to the increase in ˙OH production with the addition of H_2O_2 [15]. However, excessive H_2O_2 produces ˙OH radical might lead to a scavenger effect on the ˙OH radicals rather than a producer (see Eq. 1, 2) [14]. Hence, the overall reaction rate is deduced.

$$H_2O_2 + HO^{\cdot} \rightarrow HO_2^{\cdot} + H_2O \quad (1)$$

$$HO_2^{\cdot} + HO^{\cdot} \rightarrow H_2O + O_2 \quad (2)$$

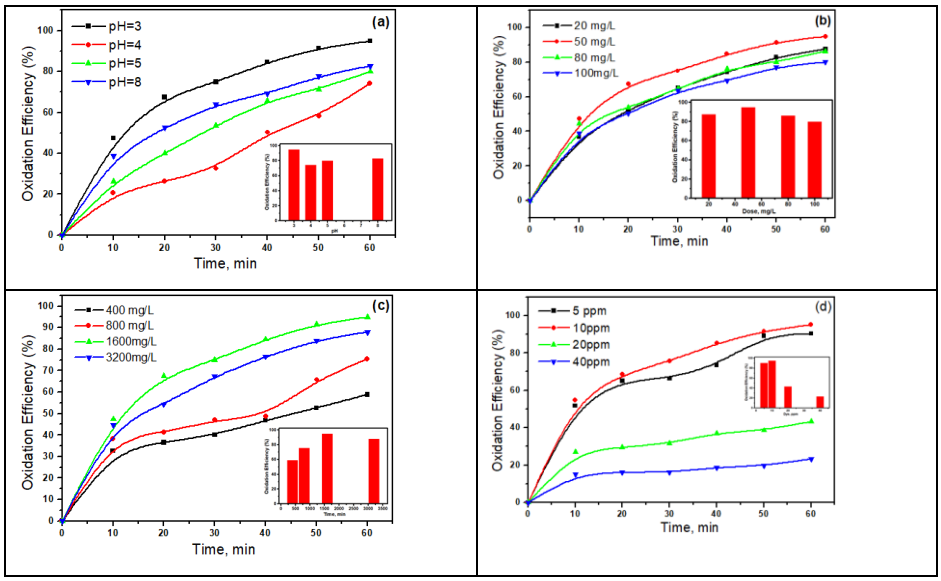

Figure 4. Effect of (a) pH (b) Dosage of photocatalyst, (c) concentration of H_2O_2, (d) (Rh-B 6G) dye Concentration, (Dye 10 ppm, H_2O_2 1600 mg/L, $Cd_{0.5}Ag_{0.5}Fe_2O_4$ 50 mg/L, pH 3.0).

3.3.4. Impact of the initial dye concentration: For the crucial practical applications, it is important to examine the dye loadings in the treatment efficiency. To evaluate that role on the photocatalytic activity, various Rh-B 6G dye concentrations (5, 10, 20, and 40 mg/L) were examined under the above-mentioned optimal circumstances conditions. Fig. 4d shows that an increase in starting dye concentration from 5 to 10 ppm improved the oxidation efficiency from 90.36 to 95.02%. However, further increase results in a steady fall to 23.29% for 40 mg/L. This could be demonstrated by the initial improvement in oxidation efficiency is probably linked to the high affinity between dye molecules and nanocomposite. But, the further increase in (Rh-B 6G) dye loading results in minimal photons absorption since the UV light could not penetrate onto the catalyst surface. As a result, the oxidation efficiency decreases [16]. Moreover, the rise in the dye color of the polluted water may also be connected to this decrease in oxidation efficiency. This dye color exerts a shadowing effect on the solution, preventing UV radiation from accessing the aqueous solution. Hence, the oxidation system's primary power source, the ˙OH radicals, are reduced, and this could lower the reaction rate as a whole [17, 5].

3.3.5. Thermal Influences on Thermodynamic and Kinetic Studies: Examining the impact of temperature on the oxidation yield and the reaction rate is crucial for practical implementation. As a result, series of experiments was studied to examine the temperature change within the range of 40–60 °C. The findings in Fig. 5a showed that the rate of reaction between the prepared ferrite and H_2O_2 rises with temperature resulting in increasing the photo catalytic oxidation of the (Rh-B 6G) dye. As a result, the yield of oxidizing species, specifically hydroxyl radicals, increases, which has a favorable effect on the oxidation and mineralization of (Rh-B 6G) [18].

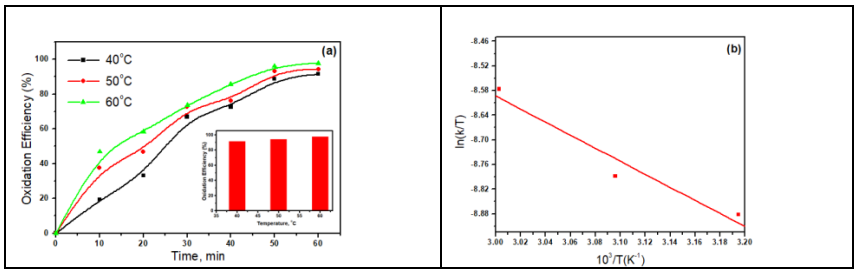

Figure 5. (a) Temperature's effect, (b) Eyring plot for photocatalytic oxidation of (Rh-B 6G) = 10 ppm with [H_2O_2] = 1600 mg/L in the presence of 50 mg/L of $Cd_{0.5}Ag_{0.5}Fe_2O_4$ ferrite at pH = 3.0.

The oxidation kinetics was investigated at different starting dye concentrations ranging from 5 to 40 ppm in order to completely comprehend the oxidation of the prepared ferrite on the dye oxidation. The kinetics of the reaction is examined using the zero, first and second reaction kinetic models. Based on the slop and intercept of the equation for the aforementioned models, the reaction kinetic constants (k0, k1, and k2) and half-life periods were determined as well as the regression coefficients (R2) are summarized in Table 1. Based on (R2) values, the photo oxidation reaction follows the first-order kinetics models [18].

Table 1. fitted kinetic rate constants for wastewater including dye oxidation*

Kinetic model	***Parameter***	***Temperature***		
		40°C	***50°C***	***60°C***
Zero-order				
($C_t = C_o - k_0t$)	k_0 (min^{-1})	0.227	0.229	0.245
	$t_{1/2}$ (min)	30.979	33.1087	33.42
	R^2	0.976	0.958	0.937
First-order	k_1 (min^{-1})	0.043	0.049	0.062
($C_t = C_o - e^{k1t}$)	$t_{1/2}$ (min)	15.949	14.065	11.03
	R^2	0.980	0.973	0.979
second-order	k_2 (L $mg^{-1}min^{-1}$)	0.01156	0.01828	0.0421
(($1/C_t$) = ($1/C_0$)	$t_{1/2}$ (min)	5.69475	4.47023	2.3385
	R^2	0.91035	0.88547	0.8501

** C_o and C_t: dye concentration at initial and time t; k_0, k_1, k_2: kinetic rate constants of zero-, first- and second-order reaction kinetic models; t: time; r^2: correlation coefficient; $t_{1/2}$ half-life time.*

The Eyring plot (Fig. 5b), which is derived from Eq. (3), is often analyzed using linear regression, allowing the thermodynamic activation parameters ($\Delta H^{\#}$ and $\Delta S^{\#}$) to be determined by calculating the slope and intercept. Table 2 lists the free energy, $\Delta G^{\#}$, and apparent activation energy, E_a, which were also computed using Equations (4) and (5)

$$\ln\frac{k}{T} = \frac{\Delta H^{\#}}{RT} + \ln\frac{K_B}{h} + \frac{\Delta S^{\#}}{R}, \quad (3)$$

Where K_B equal to the Boltzmann constant (1.38×10^{-23} JK), h equal to the Plank constant (6.626×10^{-34} Js), and R is the gas constant (8.31 J mol^{-1} K^{-1}).

$$E_a = \Delta H^{\#} + RT_{exp} \quad (4)$$

$$\Delta G^{\#} = \Delta H^{\#} - T\Delta S^{\#}, \quad (5)$$

Where, T_{exp}: average experimental temperature. *The findings presented in Table (2) indicate that the reaction under investigation is endothermic, exhibiting a decrease in randomness. The positive ΔH# and negative ΔS# values support this conclusion. The positive $\Delta G^{\#}$ values, on the other hand, indicate that the process is nonspontaneous* [4].

Table 2. Thermodynamic parameters for (Rh-B 6G) wastewater oxidation $Cd_{0.5}Ag_{0.5}Fe_2O_4$ ferrite Fenton system*

Temperature	*$k \times 10^{-2}$, min^{-1}*	*E_a, kJ mol^{-1}*	*$\Delta H^{\#}$, kJ mol^{-1}*	*$\Delta S^{\#}$, J $mol^{-1}K^{-1}$*	*$\Delta G^{\#}$, kJ mol^{-1}*
40 °C	*4.345*				
50 °C	*4.927*	*15.874*	*13.189*	*-248.75*	*93.5191*
60 °C	*6.279*				

3.3.6. Recyclability: Additionally, as the results illustrated in Fig. 6, the catalytic stability of $Cd_{0.5}Ag_{0.5}Fe_2O_4$ ferrite was assessed for the oxidation of (Rh-B 6G). Initially, after treatment such catalyst is separated with the aid of an outside magnet. The catalyst is then reused for multiple times after being separated and repeatedly cleaned with distilled water. As displayed in Fig. 8, the catalyst is used for successive four times and is initiated with washing after each cycle. The catalyst's stability and economic viability in industrial applications are assessed by the reusability test. The results showed that even though oxidation activity is declined then the fresh use; the catalyst is still possessing high catalytic activity reached to 68 % after the fourth cyclic use. This could be explained by the possibility that certain organic intermediates have occupied the ferrite active sites, covering them and preventing them from interacting with hydrogen peroxide to form •OH radicals that would otherwise attack the organic contaminants. As a result, the overall reaction rate is declined.

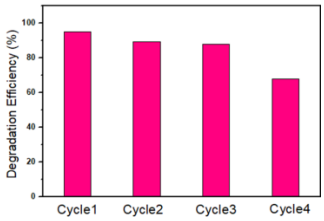

Figure 6. Recycling studies for the oxidative photo degradation of (Rh-B 6G) = 10 ppm with $[H_2O_2]$ = 1600 mg/L in the presence of 50 mg/L of $Cd_{0.5}Ag_{0.5}Fe_2O_4$ ferrite at pH = 3.0.

Conclusion: $Cd_{0.5}Ag_{0.5}Fe_2O_4$ ferrite was prepared via co-precipitation method and then used as photocatalyst for oxidation of (Rh-B 6G) dye in the presence of H_2O_2. The experimental data is well-fitted by the pseudo first-order kinetic model. At pH 3.0, 50 mg/L of produced ferrite and 1600 mg/L of hydrogen peroxide yield 94.85% efficiency. The positive value of $\Delta G^{\#}$, $\Delta H^{\#}$ and negative value of $\Delta S^{\#}$ suggesting the nonspontaneous and endothermic nature of reaction with decrease in the degree of randomness. The catalyst showed a sustainable use since it is recoverable and displayed a good catalytic activity for successive cycles.

References

[1] Y. Gao, 2015 Removal of Rhodamine B with Fe supported bentonite as heterogeneous photo-Fenton catalyst under visible irradiation, Applied Catalysis B: Environmental j,178, 29-36.
[2] G. Sharma, 2019 Highly efficient Sr/Ce/activated carbon bimetallic nano-composite for photoinduced degradation of rhodamine B, Catalysis Today, 335, 437-451.

[3] B. M. Jun, 2020 Accelerated photocatalytic degradation of organic pollutants over carbonate rich lanthanum substituted zinc spinel ferrite assembled reduced graphene oxide by ultraviolet (UV)-activated persulfate, Chemical Engineering Journal, 393, 124733.
[4] A. H. Mangood, 2023 Evaluation of synergistic approach of spinel cadmium copper nanoferrites as magnetic catalysts for promoting wastewater decontamination: Impact of Ag ions doping, Environmental Science and Pollution Research, 3, 106876–106893.
[5] M. A. Tony, 2019 Removal of the commercial reactive dye Procion Blue MX-7RX from real textile wastewater using the synthesized Fe2O3 nanoparticles at different particle sizes as a source of Fenton's reagent, *Nanoscale Advances*, 1, 4, 1362-1371.
[6] S. A. Jadhav, 2020 Magneto structural and photocatalytic behavior of mixed Ni–Zn nano spinel ferrites: visible light enabled active photodegradation of rhodamine B, Journal of Materials Science: Material in Electronics, 31, 11352-11365.
[7] N. Aladin Jasim, 2023 "Fabrication of $Zn_xMn_{1-x}Fe_2O_4$ metal ferrites for boosted photocatalytic degradation of Rhodamine-B dye," Results in Optics, 13, 100508 .
[8] R. Y. a. G. R. a. S. P. a. M. T. b. SP. Keerthana a, 2021 Pure and Ce doped spinel $CuFe_2O_4$ photocatalysts for efficient rhodamine B degradation, Environmental Research journal, 200, 111528.
[9] N. A. A. R. F. D. I. a. K. T. C. N Jamaludin2023, Photocatalytic degradation of rhodamine B dye under visible light using cerium-cobalt co-doped bismuth ferrite nanoparticles, Journal of Physics: Conference Series, 2432.
[10] M. M. Noor, 2024 The Environmental Oxidation of Acetaminophen in Aqueous Media as an Emerging Pharmaceutical Pollutant Using a Chitosan-Waste Based Magnetite Nanocomposite, 13, 3.
[11] R. H. Thabt, 2022 Synthesis, characterization and potential application of magnetized-nanoparticles for photocatalysis of Levafix CA reactive azodye in aqueous effluent, Water and Environment Journal, 36, 245-260.
[12] R. H. Thabet, 2020 Catalytic oxidation over nano-structured heterogeneous process as an effective tol for environmental remediation, IOP Conference Series: Materials Science and Engineering, 975, 012004.
[13] L. Qin, 2021 A photosensitive metal – organic framework having a fl ower-like structure for e ff ective visible light- driven photodegradation of rhodamine B †, RSC Advances, 30, 18565-18575.
[14] R. H. Thabet, 2022 Zero-Waste Approach: Assessment of Aluminum Based Waste as a Photocatalyst for Industrial Wastewater Treatment Ecology, International Journal of Environmental Research, 16, 1-19.
[15] V. Mahdikhah, 2020 Out-standing photocatalytic activity of CoFe2O4 -rGO nano-composite in degradation of organic dyes, Optical Materials, 108, 110193.
[16] E. M. F.. S. A. M.. M. A. T. Belal A. Tahoun, 2022 Development and Characterization of Conjugated Polyaniline/Co- Doped ZnO Nanocomposites for Enhanced Dye Oxidation from Wastewater, Engineering Research Journal Faculty of Engineering Menoufia University, 45, 101-110.
[17] M. A. T. S. A. E. S. I. A. A. M. K. F. Rahma H. Thabet, 2020 Catalytic oxidation over nano-structured heterogeneous process as an effective tool for environmental remediation, IOP Conference Series: Materials Science and Engineering, 97.
[18] M. A. Tony, 2023 Pattern, Forms and Bibliometric Analysis for Systematic Study of Silica-Supported Heterogeneous Solar Photocatalyst for Lanate Insecticide Abatement from Aqueous Stream, Arabian Journal for Science and Engineering, 48, 8417-8430.